PHYSICAL REVIEW B VOLUME 61, NUMBER 22 1 JUNE 2000-II

Atomic disorder in the heavy fermion superconductor $CeCu_{2+x}Si_2$

Despina Louca,[1,2] J. D. Thompson,[2] J. M. Lawrence,[3] R. Movshovich,[2] C. Petrovic,[2] J. L. Sarrao,[2] and G. H. Kwei[2]
[1]*Department of Physics, University of Virginia, Charlottesville, Virginia 22904*
[2]*Los Alamos National Laboratory, Los Alamos, New Mexico 87545*
[3]*Department of Physics and Astronomy, University of California, Irvine, California 92697*
(Received 10 April 2000)

Superconducting, magnetic, and non-Fermi-liquid-like ground states evolve in $CeCu_{2+x}Si_2$ with small changes in the Ce/Cu ratio that leave the average crystal structure unchanged. We find, however, that the local atomic structure determined by neutron pair density function analysis for a superconducting sample with $x=0.33$ is fundamentally different from a nonsuperconducting sample with $x=-0.08$. The local lattice of the Cu-deficient sample exhibits long-range atomic order, while the Cu-rich sample is intrinsically disordered. Spin-lattice coupling in the disordered lattice produces an inhomogeneous magnetic state that allows superconductivity to develop and may contribute to observed non-Fermi-liquid effects.

Since the discovery of heavy-fermion superconductivity in $CeCu_2Si_2$ (Ref. 1) and subsequently the identification of magnetic phases that appear near the superconducting boundary,[2] this material has served as a prototype of what is believed to be universal behavior in heavy-fermion materials, namely that heavy-fermion superconductivity appears near a magnetic-nonmagnetic boundary. The generally accepted view for the origin of this behavior is the coupling and competition of two primary interactions: the long-range Ruderman-Kittel-Kasuya-Yosida (RKKY) interaction that favors a magnetically ordered state and the short-range many-body Kondo interaction responsible for producing a very large effective electron mass (heavy-fermion behavior) and a magnetic singlet state. Both depend on a coupling constant $g=|J|N(0)$, with J the magnetic exchanged and $N(0)$ the density of electronic states at the Fermi energy; RKKY interactions increase as g^2 while Kondo interactions increase exponentially with g. With increasing g, Kondo interactions dominate RKKY, driving the magnetic state to a zero-temperature transition. Near this boundary, frequency- and momentum-dependent spin fluctuations associated with these interactions mediate heavy-fermion superconductivity.[3] $CeCu_2Si_2$ appears to be poised at or near a critical value of $g=g_c$, i.e., a quantum-critical point that defines a zero-temperature transition between nearly degenerate magnetic and superconducting states. The delicate balance between these two states is tipped easily by slight changes in a control parameter, e.g., Ce/Cu ratio[4] or the application of small pressures.[5]

The relationship between magnetism and superconductivity in $CeCu_2Si_2$ and related heavy-fermion systems[6] is strikingly similar to that found in the cuprate superconductors,[7] in which the crossover from a magnetic to a superconducting state is controlled by carrier density. In addition, as in the cuprates, where an unconventional linear-in-temperature resistivity appears near the magnetic-nonmagnetic boundary, unconventional thermodynamic and transport properties emerge in $CeCu_2Si_2$ as well.[8] These atypical properties are often attributed to non-Fermi-liquid (NFL) behavior. The origin of NFL behavior and its relationship to superconductivity in both the cuprates and heavy-fermion materials are currently important problems in condensed-matter physics. Some clues to this relationship in the cuprates are emerging from observations[9–11] that the crystalline structure of the cuprates is intrinsically inhomogeneous. This inhomogeneity appears to be important for superconductivity and can lead, in addition to proximity to a quantum-critical point,[12] to NFL behavior.[13]

Although superconducting T_C (~ 0.7 K) and magnetic T_N (~ 0.7 K) transition temperatures in $CeCu_2Si_2$ are approximately two orders of magnitude lower than in the cuprates, the remarkable similarities between their temperature-control parameter phase diagrams and appearance of NFL behavior suggest that, in analogy to the cuprates, atomic and/or magnetic inhomogeneities might be present in $CeCu_2Si_2$ and might play a role in its superconductivity as well. Indeed, indirect evidence for atomic inhomogeneity in $CeCu_2Si_2$ has been found from positron annihilation experiments,[14] from structural refinement of single-crystal diffraction data that suggest large Debye-Waller factors,[15] and from the appearance of a symmetry-forbidden A_{1g} phonon peak in the Raman spectrum.[16] However, in the absence of direct observation of inhomogeneity, these effects have not been considered essential for understanding the physics of $CeCu_2Si_2$, as was the case for several years with the cuprates. Motivated by these observations, we have examined the local atomic structure of superconducting and nonsuperconducting $CeCu_2Si_2$ samples by the pair density function (PDF) analysis of neutron-diffraction data. We find that, in agreement with previous structural studies,[17] the average crystal symmetry is the same for both samples; however, on a scale of 8 Å or less, the local atomic structure is homogeneous in the nonsuperconducting sample but inhomogeneous in the superconducting sample.

Two polycrystalline samples were prepared by arc melting, one with a starting Ce:Cu:Si ratio of 1:2.33:2 and one with 1:1.92:2. These will be referred to as $x=0.33$ for ''$CeCu_{2.33}Si_2$'' and $x=-.08$ for ''$CeCu_{1.92}Si_2$'' samples, respectively. The buttons were turned five times between melts to ensure chemical homogeneity. No weight loss was observed in the process. They were subsequently annealed at 900 °C in a quartz tube then crushed into powder and sub-

TABLE I. Results of the Rietveld refinement of the diffraction data collected. Note that the crystal symmetry ($I4/mmm$) is the same and the structure parameters are very similar for the two compounds. Ce is at $(0,0,0)$, Cu at $(0,\frac{1}{2},\frac{1}{4})$ and Si at $(0,0,z)$. The lattice constants are slightly smaller in the case of excess copper.

	$CeCu_{1.92}Si_2$ (20 K)	$CeCu_{2.33}Si_2$ (13 K)
Lattice Parameters	$a=4.08599(13)$ Å $c=9.9149(3)$ Å $z_{Si}=0.37969(6)$	$a=4.08441(13)$ Å $c=9.9099(3)$ Å $z_{Si}=0.37973(7)$
Volume Fraction	$CeCu_2Si_2$-99.99%	$CeCu_2Si_2$-94.27% Cu-5.73%
$U_{iso}(\times 100)$	Ce-0.260 Cu-0.343 Si-0.342	Ce-0.244 Cu-0.359 Si-0.349
Rietveld factor	4.86	4.29

jected to a final annealing for another day at 500 °C. Neutron-diffraction data were collected at several different temperatures using the glass, liquid, and amorphous materials diffractometer (GLAD) of the Intense pulsed neutron source (IPNS) at Argonne National Laboratory. The structure function, $S(Q)$ (with Q as the momentum transfer $1 < Q < 33\,\text{Å}^{-1}$) was obtained after subtracting background and correcting for absorption, multiple scattering, as well as inelastic scattering (Placzek corrections[18]). The $S(Q)$ was subsequently Fourier transformed to obtain the pair density function (PDF),[19] which provides a representation in real space of local atomic pair correlations. Diffraction data used for crystallographic Rietveld refinement were collected using the general purpose powder diffractometer (GPPD) of IPNS which offers higher resolution in d space, and the results are summarized in Table I for the two compositions. The average crystal symmetry of the primary $CeCu_2Si_2$ phase is the same, regardless of the nominal Cu concentration.[20] Structural models of the primary phase in both samples yield a stoichiometric unit cell. Models for the $x=-0.08$ with Cu site occupancy less than 1.0 yield an equivalently good χ^2 value as with full occupancy making the two models indistinguishable. For $x=0.33$, we find in addition to $CeCu_2Si_2$, the presence of 5.73% phase fraction of fcc copper.

The ac magnetic susceptibility of the two samples is shown in Fig. 1. The $x=-0.08$ sample exhibits a weak diamagnetic signal below 0.3 K and no evidence for a specific-heat anomaly at this temperature (not shown). In contrast, the $x=0.33$ sample shows bulk superconductivity and a $T_C=0.671$. Previous work suggested that the $x=-0.08$ sample exhibits a form of weak magnetism whose origins could either be antiferromagnetic or in the form of a spin-density wave,[21] and it is generally believed that it does not coexist with superconductivity.[22]

The temperature dependence of the local atomic structure for the $x=-0.08$ sample is shown in Fig. 2. Peaks in the PDF correspond to pairs of atoms centered at the average bondlength separation. The first peak at 2.4 Å corresponds to the shortest bond distance in the crystal. The intrinsic PDF peak width at 10 K is limited by quantum zero-point vibrations. By 300 K, the height of some peaks decreases by as much as 20–50 %. Part of this reduction can be accounted for by an increase in atomic thermal fluctuations with increasing temperature and in part due to the relatively low Debye temperature, ~200 K, of this material.[1] In addition to peak height reduction, peak shapes change particularly in the region from 3.5 to 7.0 Å. These changes arise from the anisotropy in thermal expansion,[23] where the a axis of this material expands nearly twice as much as the c axis with increasing temperature. Consequently, bondlengths of pair correlations from different directions might contribute to a particular peak and expand nonlinearly with temperature. Since the PDF is a powder average of a cumulative sum of all pairs, the anisotropic thermal expansion leads to peak broadening and, in some occasions, changes in peak shape.

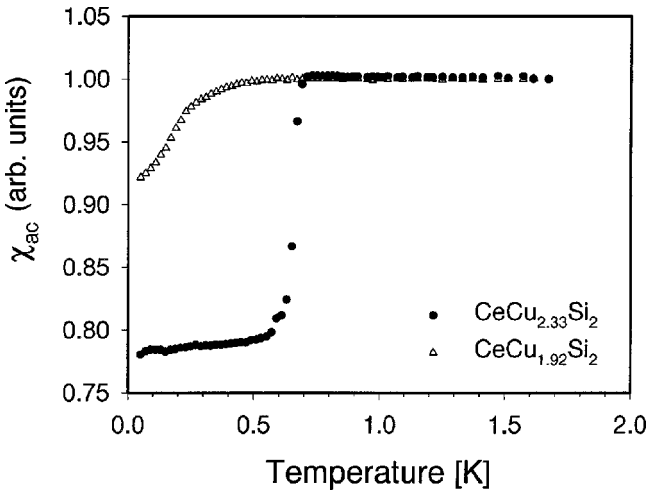

FIG. 1. ac susceptibility measurements for $x=-0.08$ (triangles) and $x=0.33$ (black circles). A bulk superconducting transition is only exhibited by the latter sample.

A model PDF for the $x=-0.08$ material is constructed using the atomic coordinates and unit cell dimensions obtained from Table I. The model PDF is calculated by summing all partial PDF's with respect to every atom in the

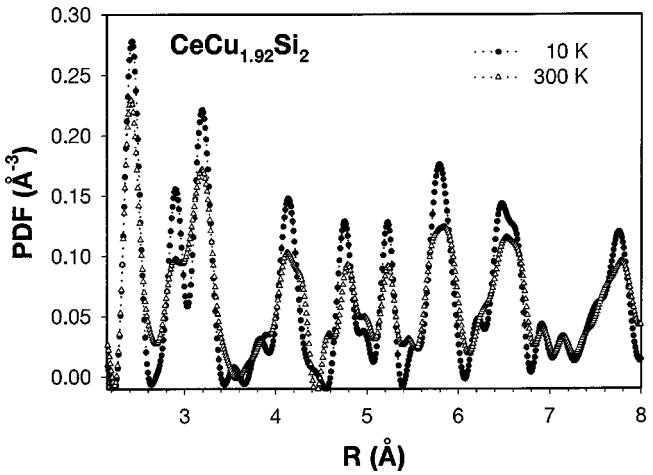

FIG. 2. The PDF's of $x=0.08$ at 10 K and 300 K. Within this temperature range, the system undergoes thermal expansion where the a axis expands more than the c axis.

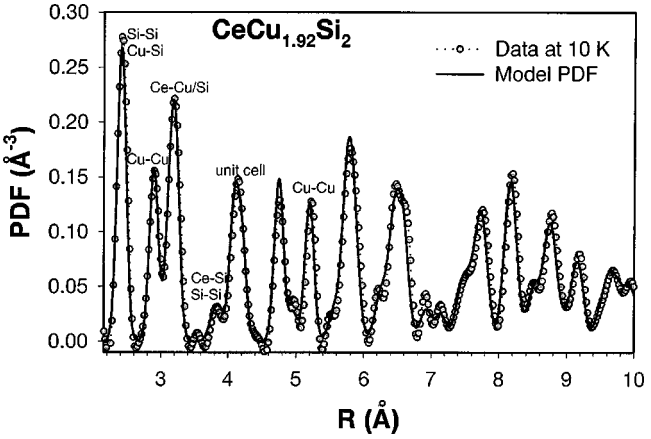

FIG. 3. The PDF for $x=-0.08$ determined at 10 K is compared to a model calculated from the average crystal structure. The agreement between the two is excellent.

lattice, and pair correlations are represented by delta functions, whose widths, σ, are broadened by convolution with a Gaussian function to simulate thermal vibrations. As shown in Fig. 3, this model gives excellent agreement with the experimentally determined PDF at 10 K. This agreement serves as a strong indication of the coherence of the local structure with the average crystal structure. It also confirms that the crystal structure of ''$CeCu_{1.92}Si_2$'' is almost perfectly periodic. By 300 K, the same model fits well to the local structure but with broader peak widths, corresponding to the increase in thermal vibrational amplitude.

The local atomic structure determined for the superconducting $x=0.33$ sample at 10 K is shown in Fig. 4 and is compared to a model for the average crystal structure. This model PDF consists of the majority phase, 94.27% $CeCu_2Si_2$, plus the second phase, fcc Cu of 5.73% as determined by Rietveld refinement of the diffraction pattern. The model peak widths were convoluted with the same σ values as in the model of Fig. 3. It is evident. however, that in contrast to the very good agreement found between the average model and experimental PDF of the $x=-0.08$, this

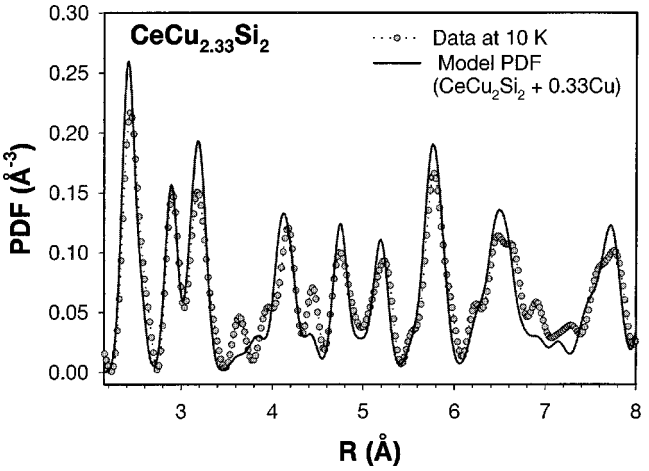

FIG. 4. The PDF for the superconducting $x=0.33$ sample at 10 K is compared to the model PDF for the average crystal structure. Several differences are observed between the model and experimental PDF's.

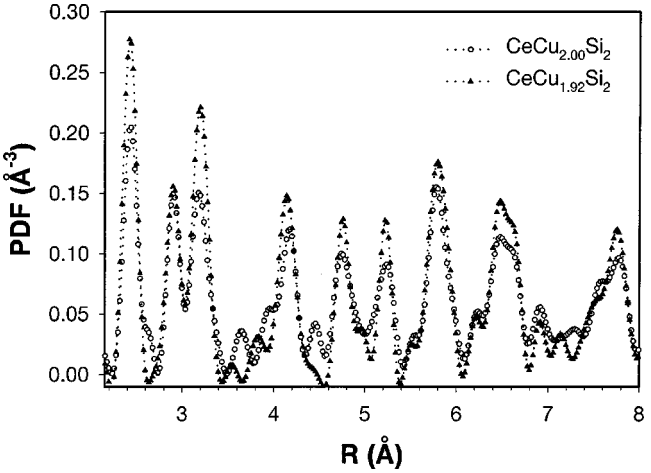

FIG. 5. The PDF's determined at 10 K for the $x=-0.08$ and $x=0.33$ with fcc Cu subtracted from the total PDF of the latter. Differences in the height and shape of several peaks are seen between the two. Their PDF's look very similar above 8 Å.

average structure model does not account as well for the local lattice of the superconducting $x=0.33$ sample.

In Fig. 5, we plot PDF's of $x=-0.08$ and $x=0.33$ where the free Cu component has been subtracted from the latter to compare their ''$CeCu_2Si_2$'' lattices. The excess free copper in $x=0.33$ does not enter the unit cell interstitially, but rather segregates as separate grains thus justifying its subtraction from the total PDF of ''$CeCu_{2.33}Si_2$.'' In PDF, by introducing a Cu atom at an interstitial site in the unit cell, new peaks at bond lengths shorter than 2.4 Å, the shortest distance in the structure, would appear. Such ''new'' peaks are not present confirming the fact that the excess Cu segregates into a second phase. Unlike the fact that the average $CeCu_2Si_2$ structure of the Cu-rich and Cu-deficient compositions is the same, in reality their local atomic structures are quite different, particularly in the region below 8 Å. Above that, the PDF's for the two samples are quite similar and also agree with the average structure (not shown). This suggests that at larger length scales the structures of the two compounds are very similar, while local atomic distortions prevalent at short length scales and leading to structural inhomogeneity in the superconducting sample are what makes the two different. As with the cuprates, it is possible that these distortions are dynamic in nature, embedded in the PDF as part of the total signal as the integration of the diffraction data occurs over a finite energy window.[24]

Although we have not formulated a model that quantitatively accounts for the local structure of the superconducting sample, the PDF data provide evidence for lattice inhomogeneity. Because of the strong volume dependence of the magnetic exchange $|J|$ in heavy fermion systems,[25] this inhomogeneity should lead to a distribution in strength of the Kondo interaction, or equivalently, a distribution in the hybridization strength between cerium localized f electron and surrounding ligand electrons. Magnetic inhomogeneity of this kind has been shown to be a possible source of NFL behavior.[26] The appearance of a spatially inhomogeneous magnetic state with increasing Cu content provides a logical explanation for the mechanism by which weak magnetism in

nonsuperconducting $CeCu_2Si_2$ is suppressed. Superconductivity, then, would be allowed to develop from a magnetically inhomogeneous state, as also implied by muon spin rotation[27] and nuclear quadrupole-resonance experiments.[28] Applying pressure to Cu-deficient samples induces superconductivity as well. PDF measurements in this case also should reveal similar local atomic inhomogeneity. These experiments are planned.

The authors are grateful to R. Modler and T. Egami for several valuable discussions. They also thank J. A. Johnson for help with GLAD and J. Richardson with GPPD. Work at the Los Alamos National Laboratory was performed under the auspices of the U.S. Department of Energy under Contract No. W-7405-Eng-36. The IPNS was supported by the U.S. Department of Energy, Division of Materials Sciences, under Contract No. W-31-109-Eng.38.

[1] F. Steglich *et al.*, Phys. Rev. Lett. **43**, 1892 (1979).
[2] G. Bruls *et al.*, Phys. Rev. Lett. **72**, 1754 (1994); R. Modler *et al.*, Physica C **206-207**, 586 (1995).
[3] N. D. Mathur *et al.*, Nature (London) **394**, 39 (1998).
[4] P. Gegenwart *et al.*, Phys. Rev. Lett. **81**, 1501 (1998); W. Assmus *et al.*, *ibid.* **52**, 469 (198).
[5] F. G. Aliev *et al.*, Solid State Commun. **45**, 215 (1983).
[6] See, for example, S. R. Julian *et al.*, J. Magn. Magn. Mater. **177-181**, 265 (1998).
[7] See, for example, *Los Alamos Symposium–1989. High Temperature Superconductivity Proceedings*, edited by K. S. Bedell, D. Coffey, D. E. Meltzer, D. Pines, and J. R. Schrieffer (Addison-Wesley, Redwood City, CA, 1990).
[8] F. Steglich *et al.*, J. Phys. Condens. Matter **8**, 9909 (1996).
[9] J. M. Tranquada, Nature (London) **375**, 561 (1995).
[10] P. C. Hammel *et al.*, Phys. Rev. Lett. **71**, 440 (1993).
[11] R. J. McQueeney *et al.*, Phys. Rev. Lett. **82**, 628 (1999).
[12] S. Chakravarty B. I. Halperin, and D. R. Nelson, Phys. Rev. Lett. **60**, 1057 (1988); see, for example, J. Schmalian cond-mat/9810041 (unpublished).
[13] N. Hasselmann *et al.*, Phys. Rev. Lett. **82**, 2135 (1999).
[14] D. Vasumathi *et al.*, Phys. Rev. B **55**, 11 714 (1997).
[15] F. Steglich *et al.*, Physica B & C **126**, 82 (1984).
[16] S. L. Cooper *et al.*, Phys. Rev. B **34**, 6235 (1986).
[17] F. Steglich, in *Theory of Heavy Fermions and Valence Fluctuations*, edited by T. Kasuya and T. Saso (Springer-Verlag, Berlin, 1985), p. 23.
[18] Multiple scattering corrections at GLAD are determined by using Ni as a standard. The inelastic corrections are determined from the approximation by G. Placzek, Phys. Rev. **86**, 377 (1952).
[19] B. H. Toby and T. Egami, Acta Crystallogr., Sect. A: Found. Crystallogr. **A48**, 336 (1992).
[20] G. H. Kwei and J. M. Lawrence (unpublished).
[21] P. Gegenwart *et al.*, Physica B **259-261**, 403 (1999).
[22] B. Wolf *et al.*, Physica B **211**, 233 (1995).
[23] R. Modler, Ph.D. thesis, Darmstadt, 1995.
[24] D. Louca *et al.*, Phys. Rev. B **60**, 7558 (1999).
[25] J. D. Thompson and J. M. Lawrence, in *Handbook on the Physics and Chemistry of Rare Earths, Vol. 19*, edited by K. A. Gschneidner, L. Eyring, G. L. Lander, and G. R. Choppin (North-Holland, Amsterdam, 1994), p. 383.
[26] O. O. Bernal *et al.*, Phys. Rev. Lett. **75**, 2023 (1995); C. H. Booth *et al.*, *ibid.* **81**, 3960 (1998); A. H. Castro-Neto *et al.*, *ibid.* **81**, 3531 (1998).
[27] R. Feyerherm *et al.*, Phys. Rev. B **56**, 699 (1997).
[28] K. Ishida *et al.*, Phys. Rev. Lett. **82**, 5353 (1999).